

NJC

Accepted Manuscript



This is an *Accepted Manuscript*, which has been through the Royal Society of Chemistry peer review process and has been accepted for publication.

Accepted Manuscripts are published online shortly after acceptance, before technical editing, formatting and proof reading. Using this free service, authors can make their results available to the community, in citable form, before we publish the edited article. We will replace this *Accepted Manuscript* with the edited and formatted *Advance Article* as soon as it is available.

You can find more information about *Accepted Manuscripts* in the [Information for Authors](#).

Please note that technical editing may introduce minor changes to the text and/or graphics, which may alter content. The journal's standard [Terms & Conditions](#) and the [Ethical guidelines](#) still apply. In no event shall the Royal Society of Chemistry be held responsible for any errors or omissions in this *Accepted Manuscript* or any consequences arising from the use of any information it contains.

PEDOT Nanostructures Synthesized in Hexagonal Mesophases

Srabanti Ghosh^a, Hynd Remita^a, Laurence Ramos^{b,c}, Alexandre Dazzi^a,
Ariane Deniset-Besseau^a, Patricia Beaunier^d, Fabrice Goubard^e, Pierre-Henri Aubert^e,
Francois Brisset^f and Samy Remita^{a, g *}

^aLaboratoire de Chimie Physique, UMR 8000-CNRS, Bât. 349, Université Paris-Sud, 91405 Orsay, France

^bUniversité Montpellier 2, Laboratoire Charles Coulomb UMR 5221, F-34095, Montpellier, France

^cCNRS, Laboratoire Charles Coulomb UMR 5221, F-34095, Montpellier, France

^dLaboratoire de Réactivité de Surface, UMR 7197-CNRS, UPMC, Université Paris 6, 75006 Paris, France

^eLaboratoire de Physicochimie des Polymères et Interfaces (LPPi), Université de Cergy-Pontoise, 95031 Cergy-Pontoise Cedex, France

^fICMMO, UMR 8182-CNRS, Bât.410-420, Université Paris-Sud, 91405 Orsay, France

^gDépartement CASER, Ecole SITI, Conservatoire National des Arts et Métiers, CNAM, 292 rue Saint-Martin, 75141 Paris Cedex 03, France

*corresponding author, e-mail: samy.remita@u-psud.fr

Keywords: PEDOT, Nanostructures, Soft templates, Liquid Crystals, Surfactants

Abstract

We describe a single step preparation of nanostructures of poly(3,4-ethylenedioxythiophene), PEDOT, in the hydrophobic domains of cationic surfactant-based hexagonal mesophases via chemical oxidative polymerization of EDOT monomers using FeCl₃ as oxidizing agent. After polymerization, the hexagonal structure of the mesophases is preserved as demonstrated by polarized light microscopy and X-ray scattering measurements.

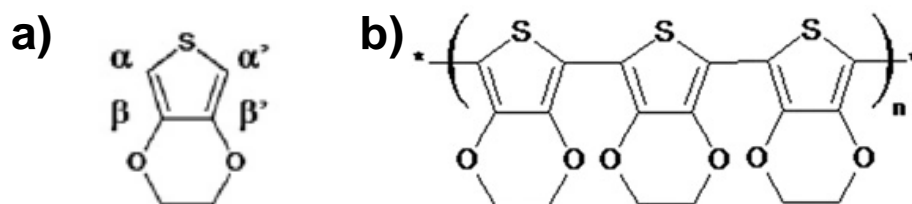
After extraction from mesophases, the chemical structure of PEDOT is confirmed by Fourier transform infrared spectroscopy. Moreover, PEDOT morphology is checked by transmission and scanning electron microscopies. PEDOT nanostructures with spindle-like or vesicle-like shapes are obtained depending on the experimental conditions. In an original way, high resolution atomic force microscopy, coupled with infrared nanospectroscopy, is used to probe the local chemical composition of PEDOT nanostructures. Finally, the as-prepared PEDOT polymers are characterized by both good thermal stability up to 200° C and relatively high conductivity value up to 0.4 S/cm as determined by thermogravimetric analysis and four probe measurements respectively.

Introduction

The development of new synthetic methodologies with an emphasis on rational control of morphology and size of nanoscale materials can facilitate revolutionary advances in science and technology.^{1,2} In this context, conjugated polymers have been the subject of intense research due to the combination of superior optoelectronic properties of semiconductors (such as high conductivity, mechanical and thermal stability) along with the advantages of organic materials (low cost, easy processing and enormous opportunities intended for structural modification).^{3,4} Recent progress established that conjugated polymers deliver great strides as active elements in electronic and optoelectronic devices as light emitting diodes for display applications, thin film transistors for low-cost and ultra-dense logic and memory circuits, photodiodes for optical information processing, photovoltaic cells for solar energy harvesting, sensors and biomedical applications.⁵⁻⁸

Among π -conjugated polymers, poly(3,4-ethylenedioxythiophene) (PEDOT) (Scheme 1) is one of the most promising conducting systems, having excellent environmental stability

and high electrical conductivity⁹⁻¹¹ which makes it ideal candidate for various applications in electronic, optical, electrochemical applications...¹²⁻¹⁴ Generally, polymerization of 3,4-ethylenedioxythiophene (EDOT) (Scheme 1) monomers, which leads to PEDOT, is based on a variety of protocols, such as wet chemical oxidation in particular by iron salts, interfacial polymerization, electrochemical polymerization or vapor phase polymerization.¹⁵⁻¹⁷



Scheme 1- Chemical structures of EDOT monomer (a) and PEDOT polymer (b). The free α and α' positions of EDOT monomers are involved during polymerization

There has been wide spread interest in the fabrication of different organic micro/nano structures with specific morphologies in a cost-effective way. Besides, significant efforts are underway to explore new techniques intended for tailoring the polymer size and shape, which in turn improve their optoelectronic properties.¹⁸⁻²¹ Importantly, a variety of lyotropic liquid crystals (LC) including hexagonal or lamellar phases have been employed for the high degree of orientational order of conducting polymers with anisotropic morphologies, which cannot be achieved using traditional bulk or solution polymerizations.^{22, 23} Nevertheless, in the particular case of PEDOT, there are only very few reports which concern the fabrication of nanostructures within LC templates.²⁴⁻²⁶ In these rare cases, electropolymerization technique was used and enabled, for instance, the fabrication of hexagonally ordered fibrillar PEDOT nanostructures into hexagonal LC.^{25, 27}

In the past years, we have employed swollen hexagonal mesophases as versatile soft templates doped with various compounds to synthesize different nanostructured materials

(such as metals, polymers or oxides) in both aqueous and oil phases.²⁸⁻³⁰ The mesophases composed of oil-swollen tubes with tunable diameters,^{31,32} which are stabilized by a monolayer of surfactant and cosurfactant molecules, have been shown to effectively control and modulate the morphology and the size of the nanostructures.³³⁻³⁵ Moreover, controlling the liquid-crystalline phase, depending on composition ranging from hexagonal, lamellar or cubic phases, can direct the dimensionality and the morphology of the nanoobjects grown *in situ*.^{36, 37} In addition to structure directing ability, the swollen hexagonal mesophases present interesting characteristics in terms of environmental safety and cost. Hence, it would be interesting to explore hexagonal mesophases assisted fabrication of conducting polymer nanostructures in particular via a chemical oxidative process. Moreover, for a facile one pot strategy and large-scale approach, it is imperative to seek the preparation of polymer nanostructures in a controlled fashion.

In the present study, we use cationic surfactant based hexagonal mesophases as templates for the preparation of PEDOT nanostructures in a simple chemical route. The idea is first to dope the mesophases with both EDOT, as monomers, and iron salt, as oxidizing species, to initiate PEDOT polymerization, and second to use the architecture of the mesophases and their hydrophilic/hydrophobic properties in order to control the morphology of the nanostructures.

Experimental section

Materials

3,4-ethylenedioxythiophene (EDOT), as monomer, iron (III) chloride, as oxidative agent, cetyltrimethylammonium bromide (CTAB) ($\geq 98\%$), sodium chloride, toluene ($> 99\%$) and pentanol ($\geq 99\%$), for hexagonal mesophases preparation, were all purchased from

Sigma-Aldrich. Ultrapure water (Millipore System, 18.2 M Ω cm) and ethanol (\geq 99% for HPLC, purchased from Sigma-Aldrich) were used as solvents, in particular for PEDOT extraction from hexagonal mesophases.

Synthetic methodology for PEDOT preparation

The hexagonal mesophases were made of a mixture of cetyltrimethylammonium bromide (CTAB) as surfactant, salted water (NaCl), toluene as oil and pentanol as cosurfactant. In a typical preparation of swollen hexagonal mesophases, 1.03 g of CTAB was dissolved in 2 mL of an aqueous solution containing salt (0.1 M NaCl). After a vigorous agitation for few minutes at 50°C, the surfactant (CTAB) was completely dissolved giving a transparent and viscous micellar solution. The subsequent addition of 2.98 mL of toluene in the micellar solution under stirring induced the formation of a white unstable emulsion. The cosurfactant (20 μ L of pentanol) was then added to the mixture which was strongly vortexed for a few minutes. This led to a perfectly translucent, birefringent and stable gel consisting in a hexagonal mesophase. This system exhibits oil in water (O/W) direct phase structure made of hexagonally packed nonpolar cylinders filled by toluene and stabilized by a monolayer of cationic surfactants and cosurfactants that can be surrounded by a continuous water domain.^{28,31,32}

According to the same procedure, other mesophases were also prepared in the presence of EDOT alone, in the presence of FeCl₃ alone or in the presence of both EDOT and FeCl₃ (always in the same proportions). EDOT and/or FeCl₃ were dissolved separately in toluene and added to the viscous micellar solution during mesophases preparation. Evidently, EDOT and FeCl₃ were never mixed together before this step in order to avoid bulk polymerization. Additionally, the swelling of the mesophases was varied by changing the volume ratio of oil over water (O/W). We varied both O/W ratio and NaCl concentration

simultaneously. For example, mesophases with O/W = 1.5 and NaCl at 0.1 M or with O/W = 2.5 and NaCl at 0.3 M were prepared at fixed EDOT concentrations.

We checked, by UV-Vis absorption spectrophotometry, that EDOT is soluble within the organic phase of mesophases up to 0.3 M. Since EDOT is only sparingly soluble in water (<0.002 M),²⁵ we conclude that EDOT is mainly present into the hydrophobic regions of the hexagonal LC (into toluene phase). One can then predict that EDOT polymerization can only be initiated in the hydrophobic region of swollen hexagonal mesophases. Moreover, since PEDOT oligomers and polymers present poor hydrophilic properties, one can also imagine that polymers growth can only take place in toluene.

While EDOT-containing mesophases remain colorless, hexagonal mesophases containing FeCl₃ salt have a yellow color (Figure S1) due to the absorption of Fe³⁺ ions (Figure S2). The simultaneous presence of EDOT and FeCl₃ into the mesophases induces a rapid change in the coloration of the systems: the initial yellow gel quickly turns into a dark blue gel which, nevertheless, remains translucent (Figure S1). This change in color indicates a chemical transformation which occurs within the mesophases and which will further be attributed to iron-induced EDOT polymerization.

In order to extract PEDOT polymers from the mesophases and for further characterization, the hexagonal mesophases were destabilized by the addition of equal volume of ethanol and water. Note that ethanol, which is less polar than water, is not only used here for mesophases destabilization, but also for enabling dissolution and dispersion of PEDOT polymers. With this protocol, a complete phase separation occurs with the organic portion in the upper phase (ethanolic phase) containing a black matter which will be identified as PEDOT. The mixture was then centrifuged and the extracted blue powder was washed with ethanol several times to remove unused reactants such as monomers and oxidants. The PEDOT was then recovered as a pure solid after full evaporation of the organic phase and was

eventually redispersed in ethanol when using solutions characterization techniques. The purity of the solid PEDOT and thus the validity of the extraction procedure were both evaluated by the measurement of the solid powder melting point.

In order to check the influence of the presence of mesophases onto the growth and then onto the final morphology of synthesized polymers, PEDOT was also synthesized in bulk solution by mixing EDOT and FeCl_3 in the same proportions in toluene solvent (without using mesophases). The black powder obtained immediately after mixing of EDOT with FeCl_3 was washed several times with ethanol and was characterized for comparison. Additionally, in order to check whether mesophases can *a posteriori* affect the morphology of soft materials such as PEDOT, these bulk polymers were mixed with pure mesophases (prepared in the absence of EDOT and FeCl_3) and then extracted using equal volumes of ethanol and water as mentioned above.

Material Characterization

The pure mesophases containing gels and the mesophases doped with EDOT monomers and/or with FeCl_3 were analyzed by small-angle X-ray scattering (SAXS) both before and after the color change of the gel. The mesophases were inserted in glass capillaries of 1.5 mm diameter and high brightness low power X-ray tube, coupled with aspheric multilayer optic (GeniX 3D from Xenocs) was employed, which delivered an ultralow divergent beam (0.5 mrad). Scatterless slits were used to give a clean 0.8 mm diameter X-ray spot with an estimated flux around 35 Mph/s at the sample position. A transmission configuration was used. The scattered intensity was collected on a two-dimensional Schneider 2D image plate detector prototype, at a distance of 1.9 m from the sample. The experimental data were corrected for the background scattering and the sample transmission. The scattering vector q can be calculated from the angle of the scattered radiation and X-ray wavelength.

Optical microscopy of gel samples before and after polymerization was performed with a Leica DMRX polarizing microscope. Additionally, the as prepared pure and doped (with both EDOT and FeCl_3) hexagonal mesophases were observed with transmission electron microscopy in a cryogenic environment (Cryo-TEM) using ultrascan 2kCCD camera (Gatan, USA), using a LaB6 JEOL JEM 2100 (JEOL, Japan) cryomicroscope operating at 200 kV. The Cryo-TEM, ensures the observation of soft nano-objects in equilibrium via a freezing process avoiding the phase transition and the possible particles aggregation which should result from drying procedures. A small amount of gel samples ($\sim 20 \mu\text{L}$) were deposited on “quantifoil”[®] (Quantifoil Micro Tools GmbH, Germany) 200 mesh holey-carbon-coated grids. After being blotted with a filter paper, the grids were quench-frozen by being rapidly plunged into liquid ethane in order to form a thin ice film avoiding water crystallization. The grids were then transferred into the microscope using a side entry Gatan 626 cryo holder cooled at -180°C with liquid nitrogen.

For chemical identification of PEDOT, attenuated total reflectance Fourier transform infrared (ATR-FTIR) spectroscopy was used. ATR-FTIR spectra of pure EDOT monomers, of solid PEDOT powders prepared in bulk solution, or of PEDOT powders obtained after extraction from the mesophases were recorded using a Bruker Vertex 70 FTIR spectrometer with diamond ATR attachment (PIKEMIRACLE crystal plated diamond/ZnSe) and a mercury-cadmium-telluride (MCT) detector with liquid nitrogen cooling system. Scanning wavelengths were varied from 4000 to 600 cm^{-1} with a 4 cm^{-1} spectral resolution using 100 repetitions scans average for each spectrum.

Thermal stability analysis of the PEDOT powders prepared in bulk solution or obtained after extraction from the mesophases was carried out by using a TGA DQ₅₀ thermogravimetric analysis (TGA) apparatus (TA instruments, USA). The test was carried out in air with a heating rate of $20 \text{ }^\circ\text{C}/\text{min}$ from 50°C to 600°C , the samples were then

isothermally treated for 30 minutes at 600°C. Differential scanning calorimetry traces were obtained using a TA Instruments Q100 DSC, using indium as the calibration standard, with heating or cooling rate of 10°C/min under nitrogen atmosphere.

UV-Visible absorption spectra of ethanolic solutions containing pure EDOT, FeCl₃ salt or dissolved PEDOT powder after extraction from mesophases were recorded using a HP8543 spectrophotometer. Ethanol solvent was always taken as reference.

The morphology eventually combined with local IR spectrum of synthesized PEDOT deposited onto solid substrate was determined by combining the classical atomic force microscopy (AFM) with free-electron laser as the IR source (AFM-IR). The AFM-IR technique combines an atomic force microscope with a pulsed infrared laser to perform spectromicroscopy beyond the conventional optical diffraction limit. We used a commercially available AFM (Veeco Explorer model), which has a visible laser focused on the cantilever, and a four quadrant detector measuring its deflection with a bench top tunable laser source.³⁸⁻
⁴⁰ For the present study, we used a commercial setup, Nano-IR (Analysis Instrument corp.) allowing us to cover the spectral range from 3600 cm⁻¹ to 1000 cm⁻¹. Usually, samples are directly deposited on the upper surface of a ZnSe prism that is transparent in the mid-infrared and the tip of the AFM remains in contact with the object. When the sample absorbs the IR laser pulse, it warms via the photothermal effect resulting in a rapid thermal expansion of the absorbing region of the sample. The thermal expansion pulse impacts the tip of the AFM cantilever and causes its oscillation. As the amplitude of oscillations is proportional to the absorption, we are able to record infrared absorption spectra at a given point and to make chemical maps by scanning the surface at a given wavelength.⁴¹ For chemical mapping, the laser wave number is fixed at a value corresponding to a specific absorption band characterizing a functional group and the tip is scanned over the sample. In this study, drops

of ethanolic solutions of PEDOT powder after extraction from the mesophases were directly deposited on the upper surface of a ZnSe prism and dried at room temperature.

For further structural study of PEDOT polymers, drops of the PEDOT ethanolic solutions after extraction from mesophases were also deposited on carbon coated grids. Transmission electron microscopy (TEM) observations were performed on a JEOL JEM 100 CXII transmission electron microscope at an accelerating voltage of 100 kV. The images were collected with a 4008×2672 pixels CCD camera (Gatan Orius SC1000).

The morphology of the PEDOT nanostructures after extraction from the mesophases was also observed by a high resolution scanning electron microscope Zeiss Supra 55 FEG-SEM. In this case, drops of PEDOT ethanolic solutions, after extraction from mesophases, were deposited on aluminium substrates.

Finally, spin-coated films were fabricated on glass slides at 1000 rpm for 60s using the PEDOT ethanolic solutions obtained after extraction from mesophases. In addition, PEDOT nanostructures obtained after extraction from mesophases were treated with NOBF_4 , as chemical oxidant, at a concentration of 10^{-2} M in acetonitrile and were then spin-coated in the same conditions. The thickness (ca. 200-500 nm thickness) of all the films (doped or non doped) was measured using a 3 Veeco Dektak 150 surface profiler. The electrical conductivity of the polymer films was measured using a Kelvin four-point probe technique implemented with Keithley 2420 system. The conductivity, ρ (S/cm) was determined using the following equation:

$$\rho = \left(\frac{\pi}{\ln(2)} \times \frac{V}{I} \times t \right)^{-1}$$

where V is the voltage difference (V), t the film thickness (cm) and I the applied current (A).

Results and discussion

PEDOT synthesis in mesophases

Swollen hexagonal mesophases, resulting from the surfactant mediated self-assembly in a quaternary system (water, surfactant, cosurfactant, and oil) serves as versatile templates for synthesizing various nanomaterials.^{28-35, 42} For PEDOT synthesis, we prepared pure mesophases at 0.1 M in NaCl with a volume ratio of oil over water (O/W) (v/v) fixed at 1.5. Mesophases with similar compositions were also prepared in the presence of EDOT at varied concentrations from 0.05 to 0.3 M. All mesophases doped with EDOT monomers up to 0.3 M remained perfectly transparent and birefringent stable gels (Figure S1).

The swollen hexagonal phases doped with increasing EDOT concentrations were studied by small angle X-ray scattering (SAXS) and appeared as representative hexagonal LC mesophases as shown Figure 1a. The hexagonal symmetry of the mesophases can be unambiguously identified by the occurrence of three Bragg peaks in the scattered intensity, whose positions are in the ratio $1:\sqrt{3}:2$. In all cases, three Bragg peaks with relative positions expected for a hexagonal phase were found to have a similar lattice parameter of 19.1 ± 0.5 nm in the absence or in the presence of EDOT monomers. This result suggests that swollen hexagonal mesophases can be used as stable soft templates providing confining media for the oxidative polymerization of EDOT. The presence of FeCl_3 (0.1 M) as chemical oxidant into the mesophases led also to yellow perfectly transparent and birefringent stable gels (Figure S1). Note that the observed yellow coloration is due to the absorption properties of FeCl_3 (Figure S2). This result also suggests that the incorporation of iron chloride salt does not destabilize the mesophases.

In the presence of EDOT monomers and FeCl_3 chemical oxidant together (in the same proportions), the mesophases turned in all cases into a translucent birefringent dark blue gel in few minutes (Figure S1). This color change indicates that a chemical reaction took place

within the mesophases, which will be further attributed to PEDOT synthesis via oxidation of EDOT by FeCl_3 . Nevertheless, at this stage of the work, the attribution of the dark blue color to PEDOT polymers trapped into the mesophases is conceivable since this color is that generally observed in literature for PEDOT polymers.²⁵

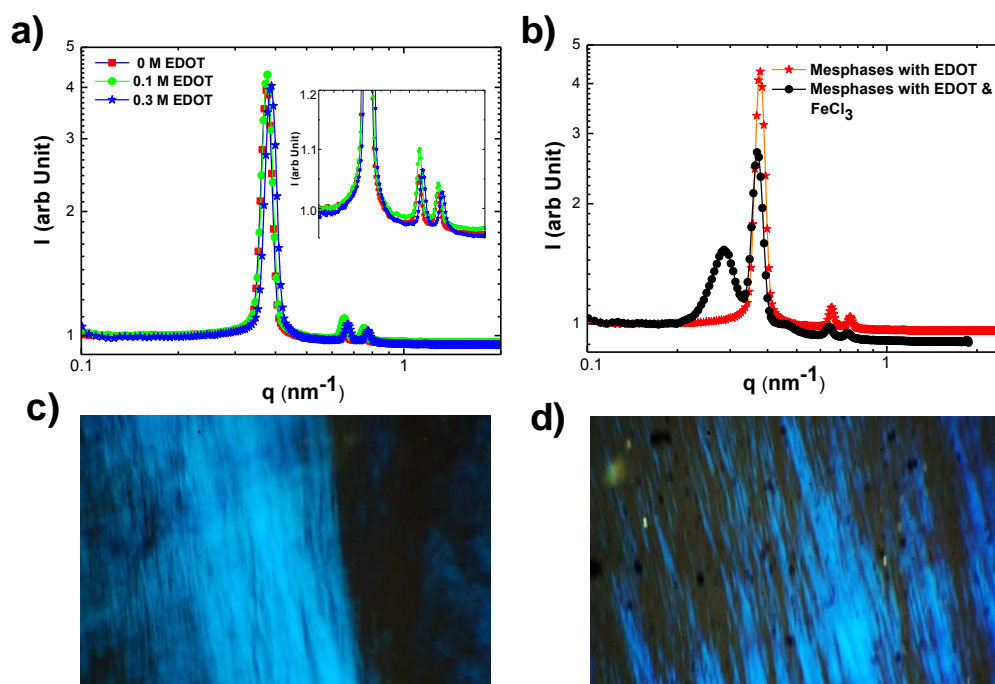


Figure 1- SAXS spectra of hexagonal mesophases at 0.1 M NaCl with increasing EDOT concentrations (0 M, 0.1 M and 0.3 M) (a); SAXS spectra of hexagonal mesophases at 0.1 M NaCl in the presence of 0.1 M EDOT with or without FeCl_3 (0.1 M) (b); Polarized light micrograph of mesophases in the absence of EDOT and FeCl_3 (c); Polarized light micrograph of doped mesophases with both 0.1 M EDOT and 0.1 M FeCl_3 (d)

The stability of the mesophases doped with both EDOT (at 0.1 M) and FeCl_3 (at 0.1 M) was also checked by SAXS measurements (Figure 1b). X-ray scattering profile displays three Bragg peaks, the positions of which are in the ratio $1:\sqrt{3}:2$. One can note that these three peaks are not displaced in comparison with those obtained in the absence of iron chloride (Figure 1a). This demonstrates that the hexagonal structure of the gels is preserved. Similar

observations were obtained when varying the experimental conditions (concentrations of both monomers and iron salts on one hand, or NaCl concentration on the other hand) indicating that whatever our experimental conditions, a relatively large degree of liquid crystalline order was preserved when mixing EDOT and FeCl₃ in oil phase of the mesophases. Nevertheless, in addition to the three previous peaks, an additional broad peak is observed in all cases around 0.288 nm⁻¹. Even if the origin of this peak is still not understood, its presence reveals the occurrence of a chemical transformation within the mesophases.

The hexagonal phases are birefringent and exhibit characteristic textures between crossed polarizing windows when the surfactant cylinders are parallel to the walls of the observation cell. The polarized optical microscopy (Figure 1c and 1d) demonstrates that the presence of EDOT and iron chloride does not affect the birefringent nature of the gels nor their texture as expected for hexagonal mesophases. However, dark spots can be observed in the presence of both EDOT and FeCl₃ (Figure 1d). This could be due to the presence of new compounds produced by the reaction of EDOT with FeCl₃ into the mesophase.

The hexagonal mesophases were also observed by cryo-TEM microscopy. Tube rod-like micelles were clearly observed in all cases, even in the presence of EDOT and FeCl₃ (Figure S3), as expected for hexagonal mesophases. These observations are obviously in very good agreement with SAXS measurements.

In order to identify the chemical nature of the products, which are responsible of the blue-dark coloration of the gels, and in order to perform morphological characterizations, the synthesized products were extracted from the mesophases.

PEDOT identification

The chemical structure of the dark blue powder extracted from mesophases was first characterized by using ATR-Fourier transform infrared spectroscopy (FTIR). The ATR-FTIR

spectrum of the product formed into the mesophases in the presence of both EDOT and FeCl_3 (both at 0.1 M) was compared with those of pure EDOT monomers and of PEDOT solid powder synthesized in bulk solutions in the absence of mesophases (Figure 2). One can note that even if the absorption bands are slightly shifted, the FTIR spectrum of the product obtained in mesophases (Spectrum 2b) is similar to that of PEDOT we synthesized in bulk solution (Spectrum 2c). These two spectra are also in good agreement with the spectrum of PEDOT obtained in literature.⁴³

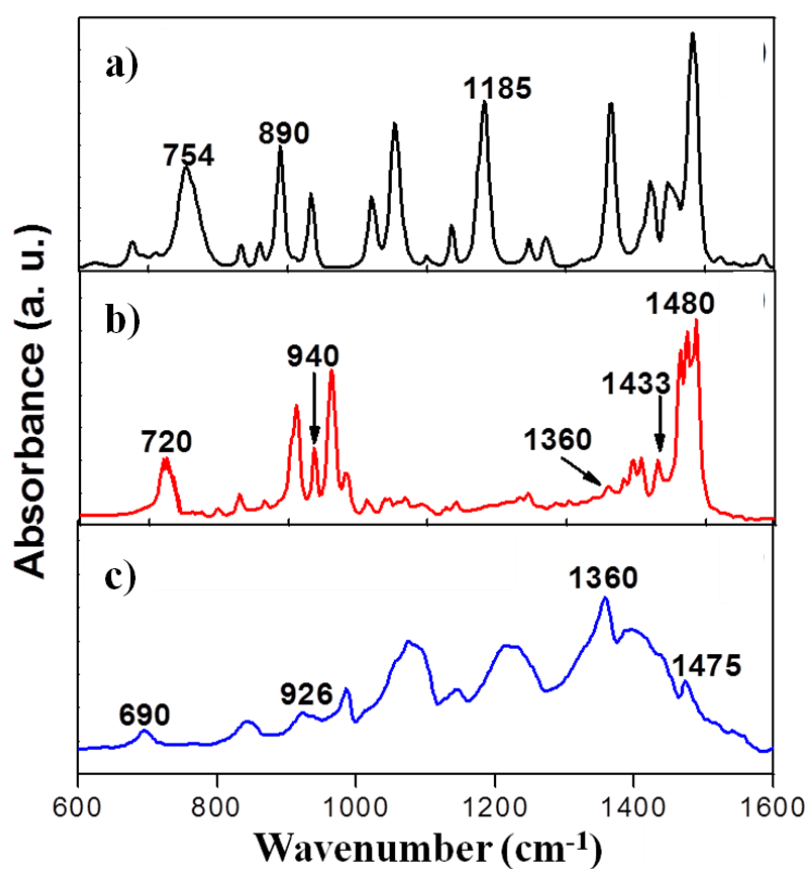


Figure 2- ATR-FTIR spectra of EDOT monomers (a), PEDOT synthesized in hexagonal mesophases at 0.1 M NaCl with EDOT (0.1 M) and FeCl_3 (0.1 M) (b) and PEDOT synthesized in bulk solution (c)

In addition, the C–H stretching band at 754 cm^{-1} observed in EDOT spectrum is not present in spectra 2b and 2c. This clearly indicates EDOT polymerization thanks to α - α' coupling and suggests PEDOT formation not only in the bulk but also into the mesophases.⁴⁴ The other vibration bands at 1480, 1433 and 1360 cm^{-1} in spectrum 2b are due to stretching modes of C=C and C-C originating from the thiophene ring, while the bands at 1299, 1243, 1141 and 1068 cm^{-1} correspond to C–O–C bond stretching in ethylene oxide group (Scheme 1). Bands at 940, 902 and 826 cm^{-1} are those of C–S bond in the thiophene ring. Note that the band at 690 cm^{-1} observed in spectrum 2c, which is related to the defects in polymer chains, is not present in the spectrum 2b of PEDOT in mesophases.

These results suggest the formation of PEDOT conjugated polymers within the confined medium of mesophases as a result of the oxidation of EDOT monomers by iron salt. Besides, the melting point of the blue-dark solid product obtained after extraction from mesophases was found to be 148°C , which is in very good agreement with the melting point values already reported for PEDOT in literature.²⁰ This definitely proves the formation of PEDOT and highlights its purity, demonstrating the validity and the efficiency of our extraction procedure. Moreover, the bands at 1185 and 890 cm^{-1} attributed to the =C–H in-plane and out-of-plane deformation vibrations of pure EDOT (Spectrum 2a) are not observed in the spectrum of PEDOT synthesized in mesophases (Spectrum 2b), nor in that of bulk PEDOT (Spectrum 2c), indicating that, in our experimental conditions, all EDOT molecules have disappeared. This could be due either to quantitative polymerization or to efficient extraction. Note that, when varying the experimental conditions (concentrations of both monomers and iron salts on one hand, or NaCl concentration on the other hand), the PEDOT nature as well as the purity of the solid powder obtained, after extraction, were always demonstrated.

After ATR-FTIR characterization, the PEDOT solid powder extracted from mesophases was dissolved in ethanol. The UV-visible absorption spectra of the PEDOT polymers synthesized at different EDOT, FeCl₃ and NaCl concentrations were then recorded as shown in Figure 3 in the case of 0.1 M in both EDOT and FeCl₃. The absorption spectrum of Figure 3 displays an absorption peak with a maximum at 390 nm together with a broad absorption band in the near IR-region of the spectrum. Such a spectrum is consistent with earlier studies concerning PEDOT.⁴⁵ Note that the near IR-region absorption band is related to bipolaron subgap transitions indicating high level of doping into the polymers.^{46, 47}

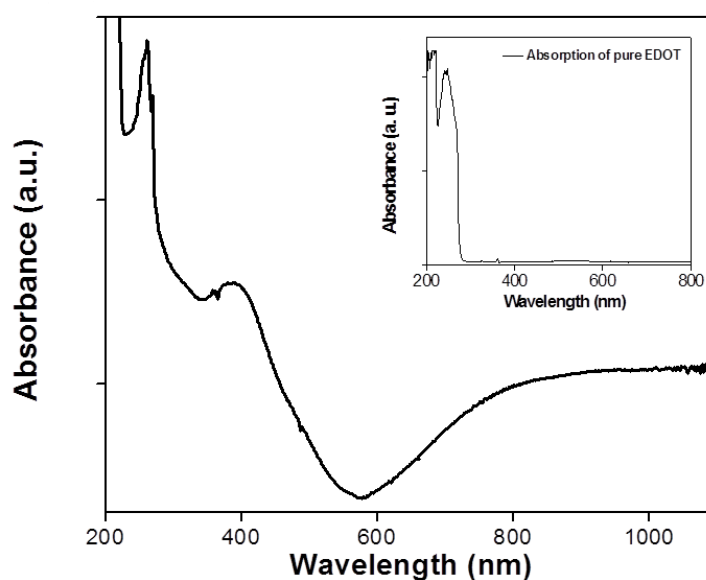


Figure 3- UV-visible absorption spectrum of an ethanolic solution of PEDOT synthesized in mesophases at 0.1 M in NaCl, 0.1 M in EDOT and 0.1 M in FeCl₃. Inset: absorption spectrum of pure EDOT monomers (0.1 M) in ethanol. The absorbancies are in arbitrary units

We can note that no absorption of EDOT is observed at 215 nm and 243 nm (compare with inset of Figure 3). This, once again, indicates the total eliminations of EDOT molecules after polymerization and extraction procedure.

PEDOT structural characterization

Drops of ethanolic solutions containing dissolved PEDOT powder were deposited on the upper surface of a ZnSe prism then dried at room temperature before AFM-IR characterization. By taking the advantages of AFM-IR technique, it is possible to obtain AFM images together with infrared spectroscopy analysis: a local infrared spectrum through the change of the wavenumber of the laser.^{48, 49} Figure 4a shows the AFM-IR spectrum of PEDOT formed in mesophases (at 0.1 M in NaCl in the presence of both EDOT and FeCl₃ at 0.1 M) and deposited onto ZnSe substrate. This AFM-IR spectrum, displayed in the 1200-1600 cm⁻¹ region, is quite similar to the FTIR spectrum of PEDOT observed on Figure 2.

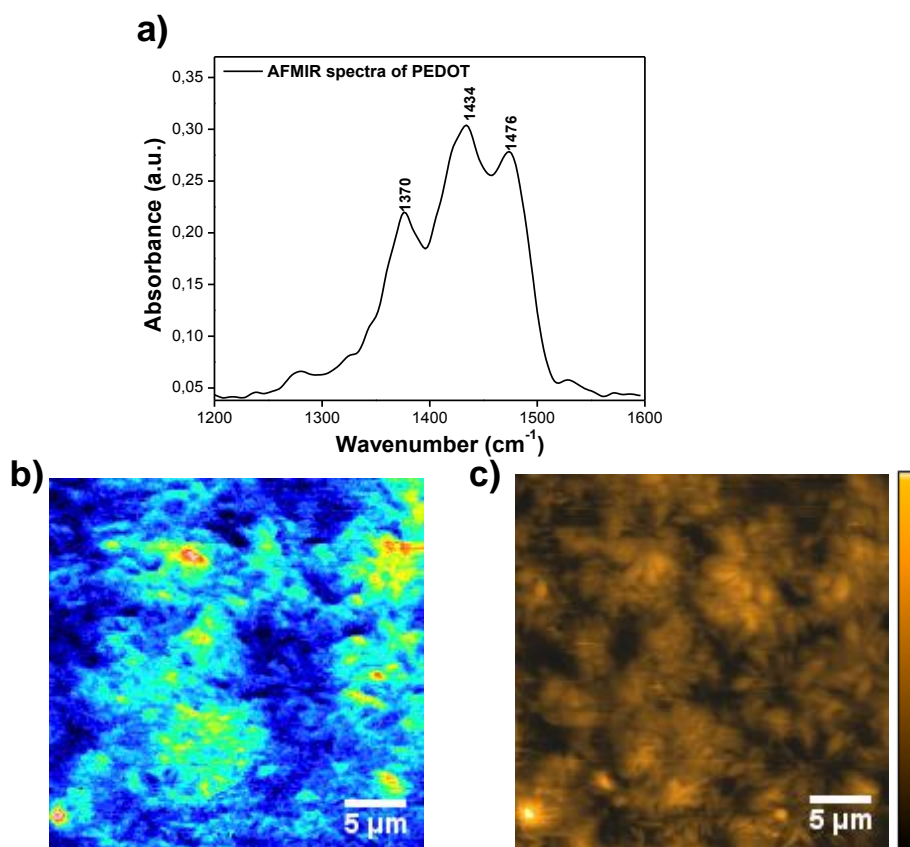


Figure 4- AFM-IR spectrum of PEDOT synthesized into the mesophases at 0.1 M in NaCl, 0.1 M in EDOT and 0.1 M in FeCl₃ (a), AFM-IR chemical map of PEDOT with the IR source tuned to the C=C band at 1476 cm⁻¹ (b) and the corresponding topographic image of PEDOT polymer (c)

The peaks around 1360 and 1476 cm^{-1} , due to C-C and C=C stretching of the quinoidal structure of the thiophene ring, indicate the effective presence of PEDOT.⁵⁰ Note that the band at 1334 cm^{-1} is relatively larger than that observed in the ATR-FTIR spectrum of PEDOT (Figure 2). This difference probably comes from the water vapor absorption which still remains during the AFM-IR measurements.

The AFM-IR technique also enables the chemical mapping of the sample. Figure 4b shows the IR absorption strength as measured by cantilever oscillations when the laser is set at 1476 cm^{-1} , while Figure 4c displays the corresponding topography. The brighter colors indicate regions of stronger IR absorption at this particular wavenumber and hence represent objects containing PEDOT polymer molecules. Looking at the corresponding topography, we notice that the brighter regions in the absorption image correspond to thicker region of the polymer. As the signal of absorption fits well with the thickness, we can assume that the objects deposited on the prism surface are only made of PEDOT. Further, we checked that if the tip is placed on the substrate without PEDOT, there is no signal.

AFM-IR technique was not only used to check the structural nature of the polymers but was also performed to provide morphological characterization of PEDOT nanostructures synthesized within mesophases. The optical images of the PEDOT polymers revealed in all the cases the presence of two types of structures: (i) well dispersed isolated ones and (ii) twisted and balled-up objects which could be the result of an aggregation (Figure S4a and b). The first objects were easily observed and characterized by AFM, while the second structures were too soft and unstable under the tip making impossible their study by AFM. Note that the twisted and balled-up objects are predominant at 0.1 M in NaCl (Figure S4a) while the isolated structures are predominant at 0.3 M in NaCl (Figure S4b) whatever EDOT and FeCl_3 concentrations (EDOT and FeCl_3 being always in the same proportions).

The isolated structures deposited onto the ZnSe substrate were observed on surface topography images of Figure 5. These images were obtained in the case of PEDOT polymers synthesized in mesophases in the presence of both EDOT and FeCl_3 (at 0.1 M) at two different NaCl concentrations (0.1 M or 0.3 M). The nanostructures obtained at 0.1 M in NaCl appear elongated with an average spindle size around 4-6 μm (Figure 5a). These nanoobjects seem to be flattened with a height of 70 nm as observed on 3D AFM image (Figure 5b). Each nanostructure which remains stable under the tip should correspond to a self assembly of PEDOT polymers which interact all together thanks to π -stacking interactions.

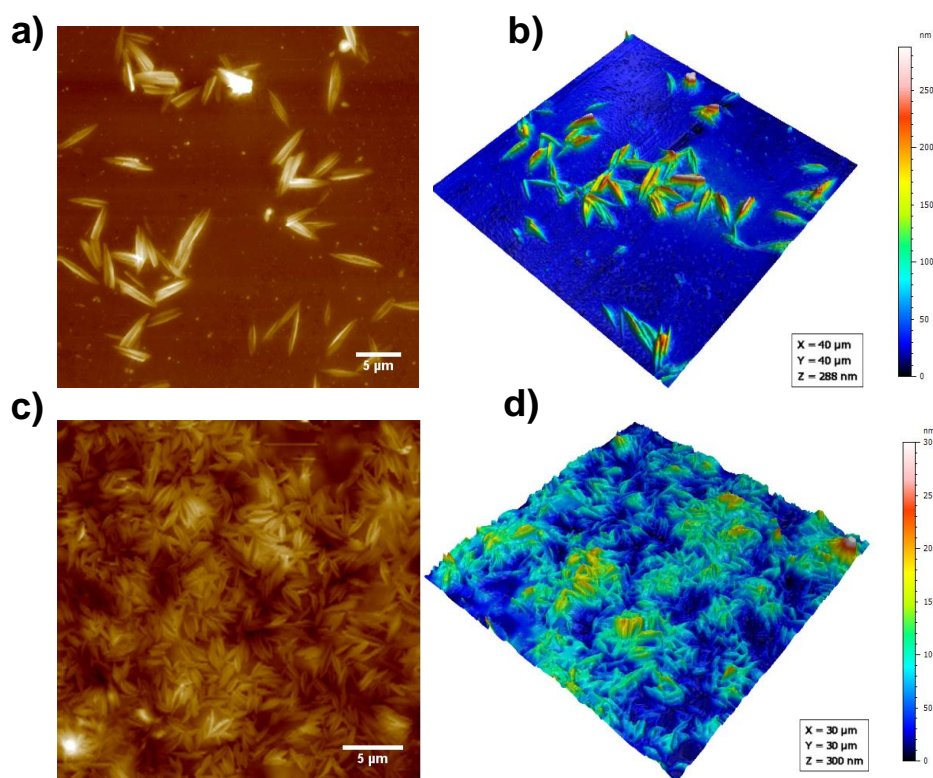


Figure 5- AFM topographic images of PEDOT extracted from mesophases and deposited onto ZnSe substrate. PEDOT synthesized using 0.1 M EDOT and 0.1 M FeCl_3 at 0.1 M NaCl (a) with the corresponding 3D AFM image (b). PEDOT synthesized using 0.1 M EDOT and 0.1 M FeCl_3 at 0.3 M NaCl (c) with the corresponding 3D AFM image (d)

In order to check whether the experimental conditions, affect the morphology of PEDOT nanostructures, we varied different experimental parameters. While EDOT and FeCl_3 concentrations (up to 0.3 M) seem to have no influence, the increase in NaCl concentration from 0.1 M to 0.3 M leads to spindle shape PEDOT objects with smaller length. In the case of PEDOT polymers synthesized in mesophases at 0.3 M in NaCl (instead of 0.1 M) in the presence of both EDOT and FeCl_3 (at 0.1 M), one can note that the length of the nanostructures is about 2 μm (Figure 5c and 5d). In addition, in comparison with the images obtained at lower NaCl concentration (Figure 5a and 5b), more PEDOT nanostructures with more regular shape are observed on the substrate (Figure 5c, in comparison with Figure 5a). Evidently, the observed difference in the number of nanostructures onto the substrate could result from the deposition procedure and from the surface coverage. However, the variation in size of the nanostructures could be due to a difference in the length of the PEDOT polymer chains when synthesized at different NaCl concentrations. Polymers may be longer when synthesized in mesophases at 0.3 M in NaCl. Probably, at higher NaCl concentrations, the diffusion of EDOT and FeCl_3 outside the micelles is slower leading to faster polymerization which evidently should lead to a higher number of polymers with smaller sizes and more regular shapes. Eventually, at higher salt concentrations, the higher ionic strength outside the micelles could also increase the concentration of EDOT into the hydrophobic region of the micelles leading to longer polymers.

In order to highlight the crucial role played by our LC templates in determining the final morphology of the polymer nanostructures and in order to demonstrate that the spindle shape as well as the balled-up structures of PEDOT result from the *in situ* growth of polymers within mesophases, we first synthesized PEDOT polymers in bulk solutions by mixing EDOT and FeCl_3 (both at 0.1 M). As expected, in these conditions, in the absence of any mesophases, an aggregated network structure of PEDOT was obtained as shown in Figure S5.

The further incorporation of these bulk PEDOT polymers into the hexagonal mesophases, followed by an extraction step, produced highly aggregated polymer structures (Figure S6). Once again, no spindle shape objects, nor balled-up structures, were observed. This definitely proves that the morphology of PEDOT nanostructures results from the confinement of the reactive species into the mesophases and of course from the further *in situ* polymerization. However, the influence of the architecture of the mesophases onto the morphology of the polymer nanostructures is not well understood. Nevertheless, by varying the experimental conditions, in particular the geometry of the mesophases, the key parameters which control the polymer structure could be identified.

In order to check the eventual influence of the substrate (ZnSe) onto the morphology of the PEDOT nanostructures and in order to characterize the twisted and balled up structures which we previously observed in the optical images (Figure S4), TEM and SEM experiments were carried out at different NaCl concentrations (0.1 M and 0.3 M). Once again and in good agreement with the previous observations on ZnSe, two kinds of nanostructures were observed on both carbon grids and aluminium substrates by both TEM and SEM techniques: (i) spindle-shape objects and (ii) balled-up objects which appear as open vesicles. This result demonstrates that the deposition procedure and that the nature of the substrate have no effect on the final morphology of the synthesized polymers. As already proposed, the kinetics of the polymerization process as well as the structure of the mesophases should have a direct impact on the size and the shape of the formed nanostructures. However for the moment, we have no clear explanation concerning the formation of the vesicles. Possibly, they could result from the lamellar packing of spindle-shaped PEDOT nanostructures.

As previously observed in the optical images (Figure S4) and as demonstrated by both SEM and TEM techniques, the open vesicles structures are predominant when PEDOT polymers are synthesized in mesophases in the presence of 0.1 M in NaCl (Figure 6), while

the spindle shape objects are predominant at higher salt concentration (0.3 M in NaCl) (Figure 7). The PEDOT vesicles obtained when polymers are synthesized in mesophases, at 0.1 M in NaCl in the presence of both EDOT and FeCl₃ at 0.1 M, present a thickness of around 40 nm and a diameter of 1 μm as observed in SEM and TEM images (Figure 6).

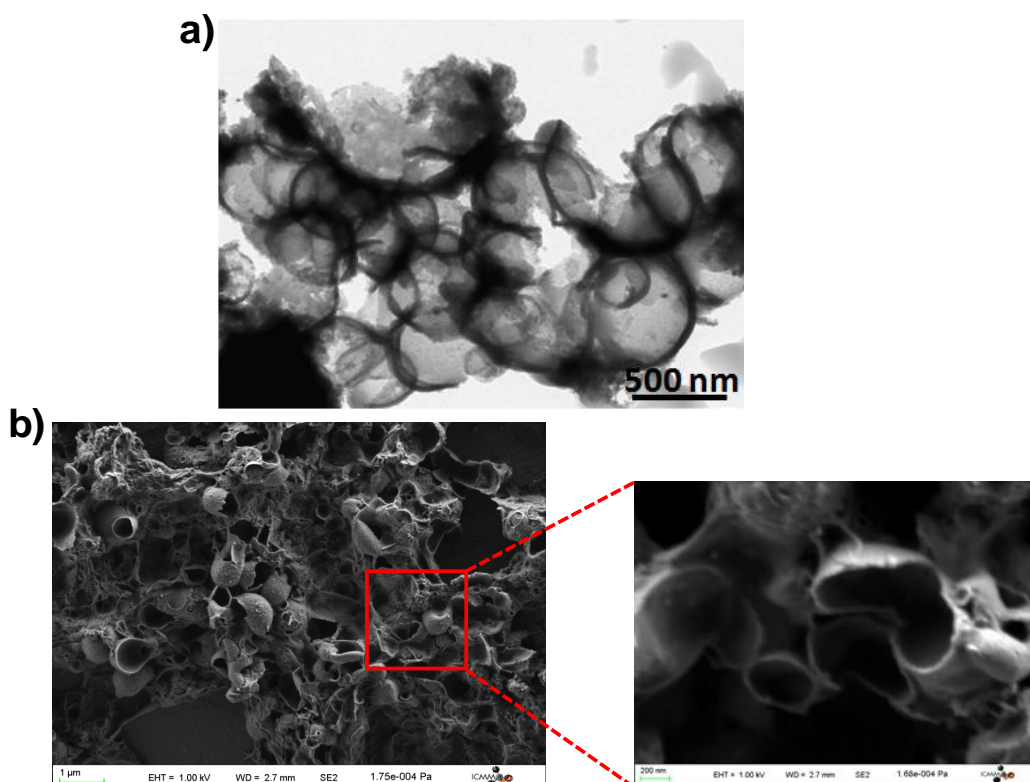


Figure 6- TEM image of PEDOT open vesicles deposited onto carbon grid (a) and SEM image (with a zoom) of the same PEDOT vesicles deposited onto aluminium substrate (b). In both cases, PEDOT polymers are synthesized into mesophases at 0.1 M in NaCl in the presence of 0.1 M EDOT and 0.1 M FeCl₃

The size of spindle-shaped PEDOT nanostructures observed in Figure 7 is in good agreement with AFM measurements (Figure 5). Indeed, a mean length of 2 μm is found for the nanoobjects of Figure 5. Nevertheless, one can note that in SEM images, these objects appear thinner than those observed by AFM. Indeed, SEM images demonstrate the flatness of

the spindle-shaped objects, the thickness of which is about few nanometers. If we suppose that the objects observed by AFM and SEM are the same, the observed morphological difference could be due to the orientation of the spindle shapes onto the different substrates. While the spindle-shaped nanostructures appear perpendicular to the aluminum substrate in SEM measurements, they remain more or less flattened onto ZnSe substrate in AFM experiments. This could be explained in terms of intermolecular interactions. Since PEDOT nanostructures are made of hydrophobic polymers, they should minimize their interaction with aluminium substrates since these latter are spontaneously covered at air by a thin hydrophilic surface layer made of aluminium oxide.

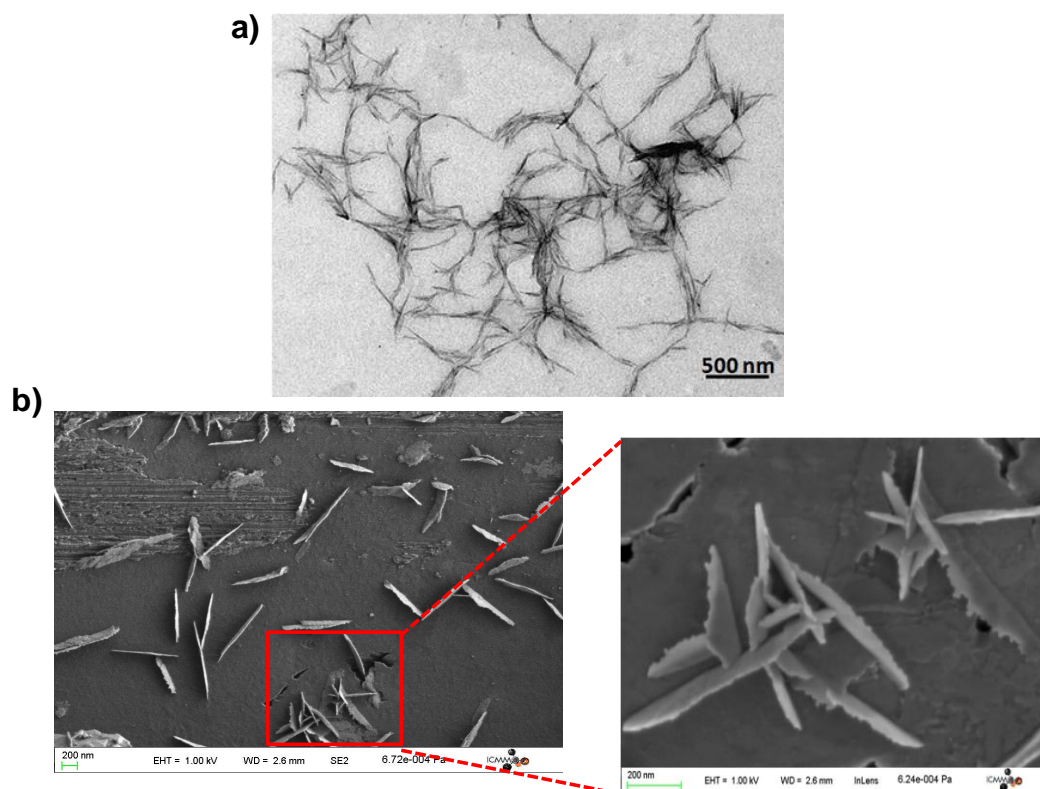


Figure 7- TEM image of spindle-shaped PEDOT deposited onto carbon grid (a) and SEM image (with a zoom) of the same PEDOT spindle shapes deposited onto aluminium substrate (b). In both cases, PEDOT polymers are synthesized into mesophases at 0.3 M in NaCl in the presence of 0.1 M EDOT and 0.1 M FeCl₃

Thermal stability and conducting properties of PEDOT

Due to its excellent thermal stability and its high electrical conductivity, PEDOT polymer is one of the most extensively used conducting materials.¹⁰ After extraction from mesophases, the thermal and electrical properties of our PEDOT polymers were then evaluated. The thermal stability of PEDOT polymers synthesized in mesophases at 0.1 M in NaCl, in the presence of EDOT and FeCl₃ both at 0.1 M, was studied by thermogravimetical analysis (TGA) and differential scanning calorimetry (DSC) in a nitrogen environment (Figure 8).

Figure 8a depicts TGA curve which enables the evaluation of the weight loss over time while the sample is heated at a constant rate. The TGA results show that PEDOT undergoes a continuous thermal degradation from 200°C until a major decomposition around 550°C. At 600°C, only a small amount (15%) of an inert residue remains. Such a result is in agreement with earlier reports concerning PEDOT.⁵¹ Indeed, it has been reported that at about 250 °C, the PEDOT weight decreases significantly and further, at higher temperatures around 350°C, other fragments due to carbon oxidation are detected. In addition, PEDOT displays decomposition pattern up to 550°C with a weight loss of about 74 wt% at 300°C and an additional 10 wt% loss at 550°C. As a consequence, the PEDOT polymers synthesized in hexagonal mesophases are characterized by a thermal stability which is as good as that of the PEDOT polymers described in literature.

Our PEDOT can be considered to be thermally stable up to 200°C. In DSC analysis, PEDOT extracted from mesophases was heated to about 200°C. A sharp endothermic transition peak was observed at 105°C (Figure 8b). We can then definitely infer that our PEDOT polymers do not display any degradation up to 200°C. In addition, pure phase of PEDOT is obtained after extraction thanks to our methodology.

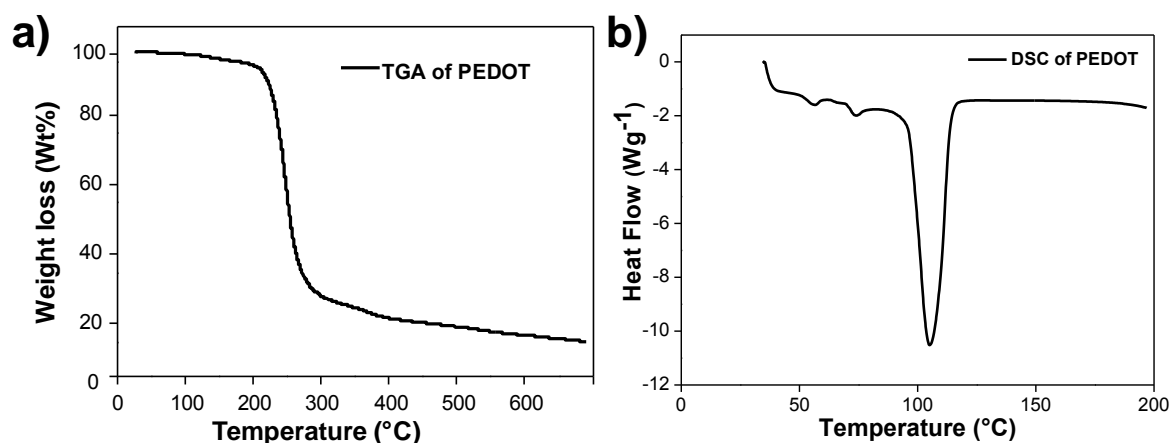


Figure 8- TGA profile (a) and DSC profile (b) of solid PEDOT nanostructures after extraction from the mesophases PEDOT polymers were synthesized in mesophases at 0.1 M in NaCl in the presence of 0.1 M EDOT and 0.1 M FeCl₃

The electrical conductivity of conjugated polymers depends significantly on their morphology, their microstructure and the number of counter ions that balance the positive doping charges carried by the conjugated polymer chains.⁵² After extraction from mesophases, after dissolution into ethanol and after spread out by spin-coating onto glass substrate, the electrical conductivity of the obtained dark blue colored PEDOT films was evaluated by using a four-point probe device. In the case of PEDOT thin films made up of polymers synthesized in mesophases at 0.1 M in NaCl, in the presence of EDOT and FeCl₃ (both at 0.1 M), the average conductivity was evaluated to 7×10^{-2} S/cm. This value is comparable with some conductivity values already reported in literature for PEDOT⁵³⁻⁵⁵ and remains higher than conductivity values of PEDOT nanostructures usually synthesized via oxidative polymerization in bulk solution.⁵⁶ Besides, the same PEDOT nanostructures obtained after extraction from mesophases were treated with NOBF₄ in acetonitrile and were

then spin-coated onto glass substrate forming, this time, transparent layers. The four probe measurements provided after doping a relatively high conductivity value up to 0.4 S/cm.

Conclusion

In the present study, we developed a simple, widely applicable, cost effective, one pot synthesis of PEDOT polymers at a submicron scale, in the confined geometry of oil-swollen tubes within a stable soft hexagonal matrix. Moreover, we showed that the PEDOT polymers prepared in mesophases can be easily extracted from their confined media and are quite simply redispersed in alcohol solutions.

We demonstrated that the morphology of PEDOT nanostructures results first from the confinement of both EDOT (monomers) and iron salt (oxidizing species) into the mesophases and second from the further *in situ* polymerization. A detailed investigation of PEDOT structure after extraction from mesophases revealed the formation of two kinds of objects: spindle-like or vesicle-like morphologies, the ratio of which depends on the experimental conditions.

PEDOT polymers synthesized into the mesophases are characterized by a very good long-term stability at air in a humid environment. Besides, we demonstrated that the as prepared PEDOT nanostructures possess good thermal stability and an electrical conductivity which is comparable with that of PEDOT polymers described in literature. Conductivity of PEDOT nanostructures was also successfully improved from 10^{-2} to 0.4 S/cm thanks to NOBF_4 doping.

Work is in due course in order to identify, thanks to the variation of mesophases geometry, the key parameters which control the growth kinetics as well as the polymer morphology. Our aim is the optimization of the preparation, within the mesophases, of

conducting materials with controlled shapes and enhanced properties. Also, we aim to use “softer” alternative physico-chemical methodologies for synthesizing PEDOT nanostructures within mesophases. Experiments using photochemistry or, more originally, radiation chemistry are in due course.

Acknowledgement

We acknowledge the RBUCE program, European Commission for a postdoctoral fellowship (Marie Curie Co-fund). We also thank Dr. Jean-Michel Guigner (IMPMC, Université Pierre et Marie Curie, France) for Cryo-TEM experiment.

Notes and References

1. J. Kao, K. Thorkelsson, P. Bai, B. J. Rancatore and T. Xu, *Chem. Soc. Rev.*, 2013, **42**, 2654–2678.
2. M. Sarikaya, C. Tamerler, A. K. Y. Jen, K. Schulten and F. Baneyx, *Nat. Mater.*, 2003, **2**, 577–585.
3. J. D. Yuen, R. Menon, E. C. Nelson, E. B. Namdas, S. Cho, S. T. Hannahs, D. Moses and A. J. Heeger, *Nat. Mater.* 2009, **8**, 572–575.
4. I. B. Martini, I. M. Craig, W. C. Molenkamp, H. Tolbert; Miyata and B. J. Schwartz, *Nat. Nanotechnol.*, 2007, **2**, 647–652.
5. F. Huang, Y. Zhang, M. S. Liu and A. K. Y. Jen, *Adv. Func. Mater.*, 2009, **19**, 2457–2466.
6. P. A. Troshin, D. K. Susarova, Y. L. Moskvina, I. E. Kuznetsov, S. A. Ponomarenko, E. N. Myshkovskaya, K. A. Zakharcheva, A. A. Balakai, S. D. Babenko and V. F. Razumov, *Adv. Func. Mater.*, 2010, **20**, 4351–4357.
7. H. Y. Chen, J. Hou, S. Zhang, Y. Liang, G. Yang, Y. Yang, L. Yu, Y. Wu and G. Li, *Nat. Photon.*, 2009, **3**, 649–653.
8. Y. Zhou, W. Huang, J. Liu, X. Zhu and D. Yan, *Adv. Mater.*, 2010, **22**, 4567–4590.
9. B. Winther-Jensen and K. I. West, *React. Funct. Polym.*, 2006, **66**, 479–483.
10. B. L. Groenendaal, F. Jonas, D. Freitag, H. Pielartzik and J. R. Reynolds, *Adv. Mater.*, 2000, **12**, 481–494.
11. A. Elschner, S. Kirchmeyer, W. Lovenich, U. Merker and K. Reuter, PEDOT: Principles and Applications of an Intrinsically Conductive Polymer, CRC Press, Taylor and Francis Group 2010, **1**, 41–63.

12. X. Wang, T. Ishwara, W. Gong, M. Campoy-Quiles, J. Nelson and D. D. C. Bradley, *Adv. Func. Mater.*, 2012, **22**, 1454–1460.
13. P. A. Levermore, L. Chen, X. Wang, R. Das and D. D. C. Bradley, *Adv. Mater.*, 2007, **19**, 2379–2385.
14. Lattach, Y.; Garnier, F.; Remita, S. *Chem. Phys. Chem.* 2012, **13**, 281–290.
15. M. Mumtaz, E. Ibarboure, C. Labrugère, E. Cloutet and H. Cramail, *Macromolecules*, 2008, **41**, 8964–8970.
16. J. L. Duvail, P. Retho, S. Garreau, G. Louarn, C. Godon and S. Demoustier-Champagne, *Synth. Met.*, 2002, **131**, 123–128.
17. S. G. Im, D. Kusters, W. Choi, S. H. Baxamusa, M. C. M. van de Sanden, K. K. Gleason, *ACS Nano*, 2008, **2**, 1959–1967.
18. W. Li, G. Zheng, Y. Yang, Z. W. Seh, N. Liu and Y. Cui, *Proc. Natl. Acad. Sci.*, 2013, **110**, 7148–7153.
19. L. Pan, G. Yu, D. Zhai, H. R. Lee, W. Zhao, N. Liu, W. H. Huiliang, C. K. Benjamin T. Y. Shi, Y. Cui and Z. Bao, *Proc. Natl. Acad. Sci.*, 2012, **109**, 9287–9292.
20. L. Youssef, A. Deniset-Besseau, J.-M. Guigner and S. Remita, *Rad. Phys. Chem.*, 2013, **82**, 44–53.
21. F. Goubard, P.-H. Aubert, K. Boukerma, E. Pauthe and C. Chevrot, *Chem. Commun.*, 2008, 3139–3140.
22. J. Kotz and S. Kosmella, *Curr. Opin. Colloid Interface Sci.*, 1999, **4**, 348–353.
23. B. -G. Kim, E. J. Jeong, J. W. Chung, S. Seo and B. K. J. Kim, *Nat. Mat.*, 2013, **12**, 659–664.
24. H. P. Hentzel and E. W. Kale, *Curr. Opin. Colloid Interface Sci.*, 2003, **8**, 164–178.
25. J. F. Hulvat and S. I. Stupp, *Adv. Mater.*, 2004, **16**, 589–592.

26. H. Goto, *J. Mater. Chem.*, 2009, **19**, 4914–4921.
27. J. F. Hulvat and S. I. Stupp, *Angew Chem. Int. Ed.*, 2003, **42**, 778–781.
28. G. Surendran, M. S. Tokumoto, E. Pena dos Santos, H. Remita, L. Ramos, P. J. Kooyman, C. V. Santilli, C. Bourgaux, P. Dieudonné and E. Prouzet, *Chem. Mater.*, 2005, **17**, 1505–1514.
29. F. Ksar, L. Ramos, B. Keita, L. Nadjjo, P. Beaunier and H. Remita, *Chem. Mater.*, 2009, **21**, 3677–3683.
30. A. Lehoux, L. Ramos, P. Beaunier, D. B. Uribe, P. Dieudonné, F. Audonnet, A. Etcheberry, M. José-Yacaman and H. Remita *Adv. Funct. Mater.*, 2012, **22**, 4900 – 4908.
31. E. Pena dos Santos, M. S. Tokumoto, G. Surendran, H. Remita, C. Bourgaux, P. Dieudonné, P. Prouzet and L. Ramos, *Langmuir*, 2005, **21**, 4362–4369.
32. L. Ramos and P. Fabre, *Langmuir*, 1997, **13**, 682–686.
33. G. Surendran, G. Apostolescu, M. Tokumoto, E. Prouzet, L. Ramos, P. Beaunier, P. J. Kooyman, A. Etcheberry and H. Remita, *Small*, 2005, **1**, 964–967.
34. F. Ksar, G. Surendran, L. Ramos, B. Keita, L. Nadjjo, E. Prouzet, P. Beaunier, A. Hagège, F. Audonnet and H. Remita, *Chem. Mater.*, 2009, **21**, 1612–1617.
35. P. F. Siril, L. Ramos, P. Beaunier, P. Archirel, A. Etcheberry and H. Remita, *Chem. Mater.*, 2009, **21**, 5170–5175.
36. H. P. Hentze and E. W. Kaler, *Chem. Mater.*, 2003, **15**, 708–713.
37. T. M. Dellinger and P. V. Braun, *Chem. Mater.*, 2004, **16**, 2201–2207.
38. A. Dazzi, R. Prazeres, F. Glotin and J. M. Ortega, *Opt. Lett.*, 2005, **30**, 2388–2390.
39. C. Policar, J. B. Waern, M. -A. Plamont, S. Clède, C. Mayet, R. Prazeres, J. -M. Ortega, A. Vessières and A. Dazzi, *Angew. Chem. Int. Ed.*, 2011, **50**, 860 –864.

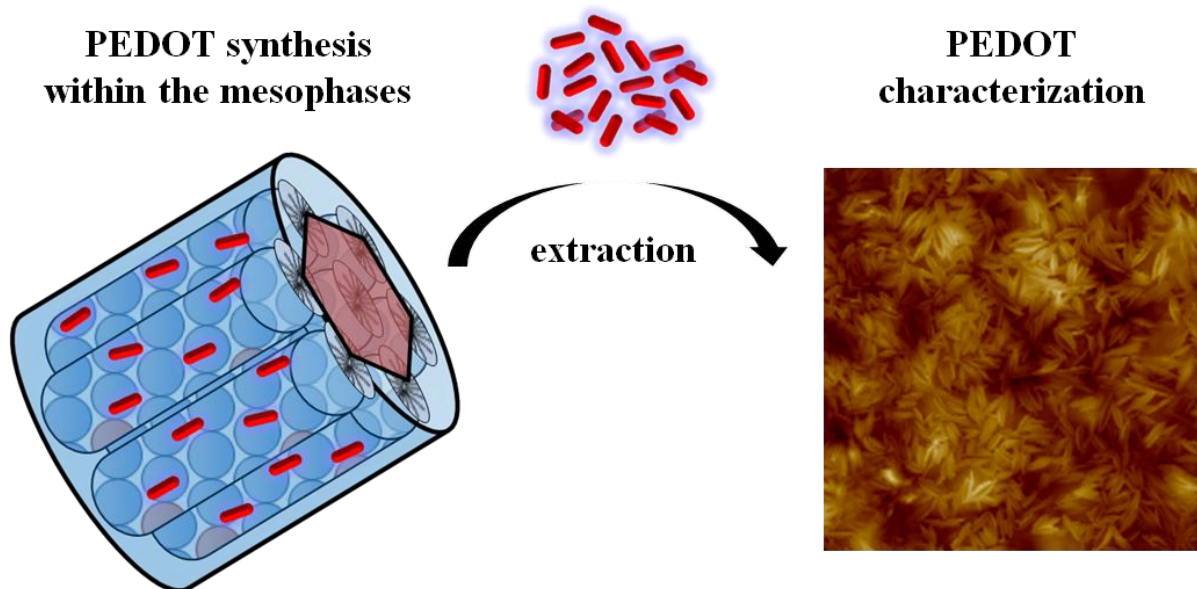
40. Dazzi, A.; Prater, C. B.; Hu, Q.; Chase, D. B.; Rabolt, J. F.; Marcott, C. *Appl. Spectrosc.* 2012, **66**, 1365-1384.
41. A. Dazzi, F. Glotin and R. Carminati, *Appl. Phys.*, 2010, **107**, 124519–124522.
42. J. C. Loudet, P. Barois and P. Poulin, *Nature*, 2000, **407**, 611–613.
43. C. Kvarnström, H. Neugbauer, S. Blomquist, H. J. Ahonen, J. Kankare and A. Ivaska, *Electrochim. Acta*, 1999, **44**, 2739–2750.
44. J. W. Choi, M. G. Han, S. G. Oh and S. S. Im, *Synth. Met.*, 2004, **141**, 293–299.
45. M. Lapkowski and A. Proń, *Synth. Met.*, 2000, **110**, 79–83.
46. A. Laforgue and L. Robitaille, *Macromolecules*, 2010, **43**, 4194 – 4200.
47. S. Garreau, J. L. Duvail and G. Louarn, *Synth. Met.*, 2002, **125**, 325–329.
48. C. Prater, K. Kjoller, D. Cook, R. Shetty, G. Meyers, C. Reinhardt, J. Felts, W. King, K. Vodopyanov and A. Dazzi, *Microsc. Anal.*, 2010, 5–8.
49. J. R. Felts, K. Kjoller, M. Lo, C. B. Prater and W. P. King, *ACS Nano*, 2012, **6**, 8015–8021.
50. M. Lapkowski and A. Proń, *Synth. Met.*, 2000, **110**, 79–83.
51. J. S. Kim, F. Cacialli, R. H. Friend, R. Daik and W. J. Feast, *Synth. Met.*, 1999, **102**, 1065–1066.
52. X. Crispin, S. Marciniak, W. Osikowicz, G. Zotti, A. Denier van der Gon, W. F. Louwet, M. Fahlman, L. F. Groenendaal, D. Schryver and W. R. Salaneck, *J. Polym. Sci. B*, 2003, **41**, 2561–583.
53. B. H. Jones, K-Y. Cheng, R. J. Holmes and T. P. Lodge, *Macromolecules*, 2012, **45**, 599–601.
54. S. E. Nair, Hsiao and S. H. Kim, *Chem. Mater.* 2009, **21**, 115–121.

55. K. E. Aasmundtveit, E. J. Samuelsen, L. A. A. Pettersson, O. Inganäs, T. Johansson and R. Feidenhans, *Synth. Met.*, 1999, **101**, 561–564.
56. Y.-H. Ha, N. Nikolov, S. K. Pollack, J. Mastrangelo, B. D. Martin and R. Shashidhar, *Adv. Func. Mater.*, 2004, **14**, 615–622.

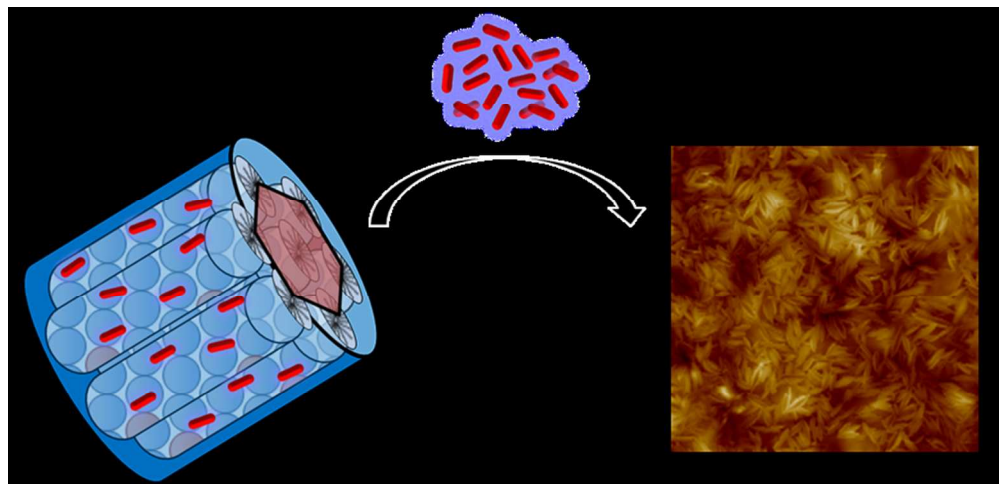
Table of Contents

PEDOT Nanostructures Synthesized in Hexagonal Mesophases

Srabanti Ghosh^a, Hynd Remita^a, Laurence Ramos^{b,c}, Alexandre Dazzi^a,
Ariane Deniset-Besseau^a, Patricia Beaunier^d, Fabrice Goubard^e, Pierre-Henri Aubert^e,
Francois Brisset^f and Samy Remita^{a, g *}



Anisotropic conducting PEDOT polymers are prepared within hexagonal mesophases according to an original one-pot synthesis and are characterized after extraction.



165x79mm (150 x 150 DPI)